Irreversible field-induced magnetic phase transitions and properties of Ho_3Co

2005 J. Phys.: Condens. Matter 17 3445

(http://iopscience.iop.org/0953-8984/17/21/034)

INSTITUTE OF PHYSICS PUBLISHING JOURNAL OF PHYSICS: CONDENSED MATTER

J. Phys.: Condens. Matter **17** (2005) 3445–3462 doi:10.1088/0953-8984/17/21/034

Irreversible field-induced magnetic phase transitions and properties of Ho_3Co

N V Baranov[1,2], T Goto[3], G Hilscher[4], P E Markin[1,2], H Michor[4], N V Mushnikov[1], J-G Park[5] and A A Yermakov[1,2]

[1] Institute of Metal Physics, Russian Academy of Science, 620219 Ekaterinburg, Russia
[2] Institute of Physics and Applied Mathematics, Ural State University, 620083 Ekaterinburg, Russia
[3] Institute for Solid State Physics, University of Tokyo, Kashiva-shi, Chiba-ken 277-8581, Japan
[4] Institut für Festkörperphysik, TU Wien, A1040 Wien, Austria
[5] Department of Physics and Institute of Basic Science, SungKyunKwan University, Suwon 404-746, Korea

Received 7 March 2005, in final form 12 April 2005
Published 13 May 2005
Online at stacks.iop.org/JPhysCM/17/3445

Abstract

The results of magnetic susceptibility, magnetization, electrical resistivity and specific heat measurements performed on Ho_3Co single crystals show that this compound exhibits two different antiferromagnetic structures: AF_{II} at 8 K $< T <$ 22 K and AF_I below $T_t \approx 8$ K. Below the Néel temperature $T_N = 22$ K the application of a magnetic field along the main crystallographic directions induces magnetic phase transitions which are accompanied by giant magnetoresistance. At $T < T_t$ the field-induced phase transitions along the ***c***- and ***b***-axes are found to be irreversible, and a small ferromagnetic component is observed along the ***a***-axis. These peculiarities are associated with the non-Kramers character of the Ho ion and with the presence of a complex incommensurate magnetic structure of Ho_3Co below T_N. The temperature coefficient of the electrical resistivity for Ho_3Co above T_N over a wide temperature range is found to differ from that observed for other R_3Co compounds. Such a behaviour is attributed to the presence of an additional contribution to the conduction electron scattering by spin fluctuations induced by f–d exchange in the itinerant d-electron subsystem. The value of this extra contribution and its temperature range is suggested to depend on the spin value of the R ion. The excess of the effective magnetic moment per R ion, which is observed in Ho_3Co and in other R_3M type compounds, is also attributed to spin fluctuations induced by f–d exchange.

1. Introduction

The intermetallic compound Ho_3Co belongs to the R_3M family with the highest rare-earth content within rare-earth–d-transition-metal binary systems. They crystallize in a low

symmetry orthorhombic structure of the Fe_3C type (space group *Pnma*) [1, 2], which forms only with d-metals having an almost filled d-band (Co, Ni, Rh). The rare-earth ions occupy two non-equivalent crystallographic positions of 4c and 8d with the local symmetry *m* and $\hat{1}$, respectively. The M atoms are located within trigonal prisms formed by the R ions.

The measurements of the magnetization, electrical resistivity and specific heat performed for some R_3Co compounds on polycrystalline samples [3, 4] and on single crystals [5–15], as well as neutron diffraction investigation [16–20], have revealed several anomalous features, which may be summarized as follows:

(i) Co as well as other d-transition metals in R_3M compounds do not possess a magnetic moment because of the strong hybridization of d-states of the transition metal with 5d-states of the rare earth and the large distance (∼0.4 nm) between neighbouring M atoms;
(ii) the magnetic moments of R atoms in R_3M form complex non-collinear antiferromagnetic (AF) or ferromagnetic (F) structures which result from competition between RKKY exchange interaction and the influence of the low symmetry crystal electric fields;
(iii) because of the complex magnetic structures the magnetization process in the ordered state of R_3M reveals a rich variety of field-induced phase transitions, which are accompanied by a giant magnetoresistance effect.

Moreover, some unusual features in the behaviour of the specific heat and electrical properties were observed for R_3M compounds. In particular, the coefficient of the electronic specific heat for Gd_3M was found to be about one order higher ($\gamma = 100$–170 mJ mol^{-1} K^{-2} than that obtained for isostructural Y_3M compounds ($\gamma = 11$–15 mJ mol^{-1} K^{-2}) [9, 21–24]), while γ-values for pure Gd and Y are close to each other ($\gamma \sim 6.4$ and 7.9 mJ mol^{-1} K^{-2}, respectively [25]). The giant enhancement of γ for Gd_3M cannot be ascribed to a possible contribution from 4f-electrons of Gd to the density of electronic states (DOS) at the Fermi level or to some peculiarities of the electronic structure of Gd_3M. According to XPS spectroscopy studies [26] the valence bands of R_3M with other rare-earth elements and yttrium are similar; as with the 4f-states of Gd, they are located far below the Fermi level. Distinctive features of the electronic structure of R_3M compounds are the substantial narrowing of the M d-band in comparison with pure transition metals and hybridization of M d-states with 5d-states of R ions (4d-states in the case of Y) [26]. For the R–Co intermetallics the following two opposite tendencies are known: the magnetic moment of Co ions decreases with increasing R content, while the energy of the f–d exchange interaction increases [27]. Therefore, in R_3M compounds having the maximal R concentration, the f–d-interaction may be very important despite the fact that the d–d exchange is small and the d-band is not split. The exchange field that arises from localized 4f-electrons of the R ion should lead to polarization of 5d-electrons on the same R ion and then spin fluctuations are induced in the d-electron subsystem of M ions through the R 5d–M d hybridization. In this case the local amplitude of spin fluctuations and, consequently, their effect upon different physical properties, is expected to depend on the spin value of the R ion. Therefore, the great difference in γ for Gd_3M and Y_3M compounds results apparently from the huge contribution due to spin fluctuations induced by Gd in the d-electron subsystem of the M transition metal via f–d exchange [21–23]. The significant influence of the spin fluctuation contribution may cause an excess of the effective magnetic moment, which was revealed for different R_3M compounds [8, 28, 29], as well as the peculiar behaviour of the electrical resistivity of R_3M compounds above their ordering temperatures [8, 9, 15, 21, 26, 28].

The magnetic properties of Ho_3Co were investigated in the early 1970s on polycrystalline samples in quasi-static [3] and pulse [4] fields. The magnetic state of this compound was then determined to be antiferromagnetic below $T_N = 24$ K. The magnetization measurements of polycrystalline samples have revealed metamagnetic-like behaviour with an appreciable

hysteresis. A recent study of a Ho_3Co single crystal has shown a significant anisotropy of the magnetization process along the main crystallographic directions [29]. Field-induced phase transitions were observed along the ***a***- and ***b***-axes, while the magnetization process along the ***c***-axis was considered to be typical for ferromagnetic materials. However, according to the neutron diffraction measurements performed on Ho_3Co powder as well as single-crystalline specimens, the complex antiferromagnetic ordering appears below $T_N \sim 22$ K, which is followed by the transformation of the AF structure at $T_t \sim 9$ K [20].

In this study, we have undertaken detailed investigations of magnetic, thermal and transport properties of Ho_3Co on single-crystalline samples in order to reveal the origin of formation of unusual magnetic states in the R_3M family.

2. Experimental details

The Ho_3Co compound was obtained by arc melting in a helium atmosphere using holmium and cobalt of 99.9 and 99.99% purity, respectively. Single crystals were grown by the Bridgman technique in a resistive furnace. The phase purity of the single crystals was checked by a metallographic method. The content of foreign phases was estimated to be less than 3%. The Laue patterns obtained from different sides of the single crystals were tested carefully for the presence of satellite reflections from other crystal grains. The samples were then cut along the main crystallographic directions [100] (***a***), [010] (***b***) and [001] (***c***).

The magnetization measurements were made with a vibrating sample magnetometer up to the fields of 7 T and in pulsed fields up to 42 T by an induction method. The ac and dc magnetic susceptibility was measured by using a SQUID magnetometer (MPMS-5XL, Quantum Design, USA). The measurements of electrical resistivity were performed on $1 \times 1 \times 5$ mm^3 samples with the long side parallel to one of the main crystallographic directions using the four-contact technique. The specific heat of Ho_3Co was measured on a single crystal with a mass of about 300 mg by an adiabatic method.

3. Results and discussion

3.1. Low-field magnetization and susceptibility

Figure 1(a) displays temperature dependences of the magnetization measured with increasing temperature along the main crystallographic axes under a field of 0.005 T. Before the measurements the sample was cooled down from 40 to 2 K in zero magnetic field (ZFC regime). The maximum of the magnetization observed along the ***a***- and ***c***-axes at ∼22 K is, we think, due to the phase transition from paramagnetic to antiferromagnetic (AF) states. This temperature is close to the value of T_N previously obtained on a polycrystalline sample by Feron *et al* [3]. As can be seen in figure 1, all the curves also exhibit a pronounced maximum at the temperature $T_t \approx 8$ K, which indicates a change of the magnetic structure with decreasing temperature. As is shown in [20] by neutron diffraction measurements, the magnetic structure in the temperature interval $T_t < T < T_N$ can be described by two wavevectors $\boldsymbol{k}_1 = (0\ 0\ 0)$ and $\boldsymbol{k}_2 = (0.15\ 0\ 0)$, while on decreasing the temperature below T_t the magnetic structure exhibits a more complicated character. The additional peaks associated with the second and third harmonics of $\boldsymbol{k}_2$ were found to appear on the neutron diffraction pattern at $T < T_t$. Thus, both the temperature dependences of the magnetization in low fields and the neutron diffraction study of Ho_3Co indicate the presence of two different antiferromagnetic structures: the AF_I structure below $T_t \approx 8$ K and AF_{II} at $T_t < T < T_N$. It should be noted that two anomalies of the magnetic susceptibility associated with the magnetic ordering at $T = 35$ K

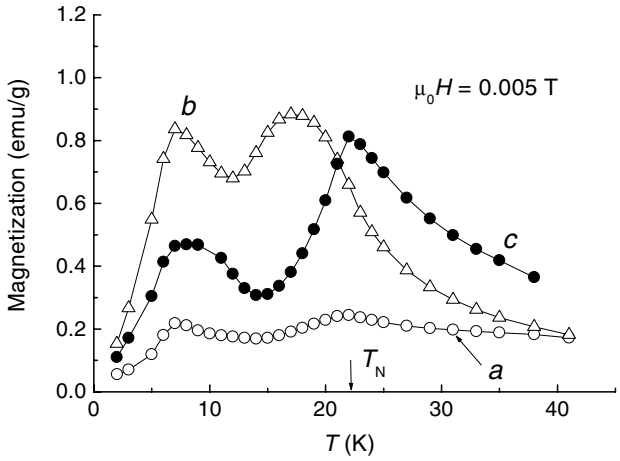

Figure 1. Temperature dependences of magnetization measured along the main crystallographic axes at $\mu_0 H = 0.005$ T.

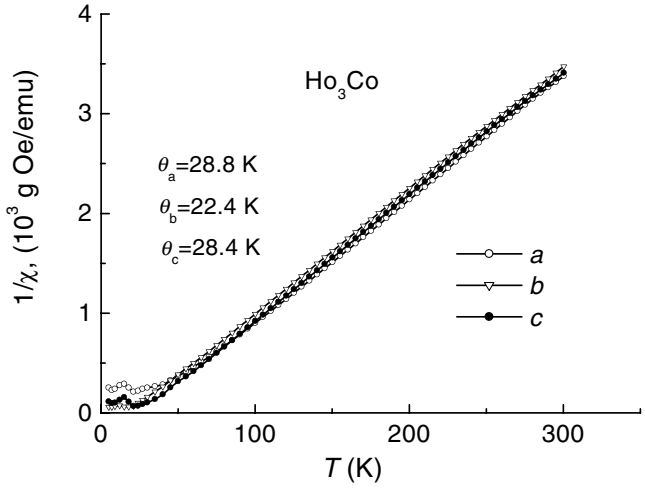

Figure 2. Temperature dependences of the inverse susceptibility measured along ***a***-, ***b***-and ***c***-axes of the Ho_3Co single crystal.

and a reorientation at 25 K were also observed for another Ho-based compound Ho_3Rh with the same crystal structure [30].

The temperature dependences of the reciprocal susceptibility along the ***a***-,***b***- and ***c***-axes are presented in figure 2. The variation of the reciprocal susceptibility is found to obey the Curie–Weiss law at temperatures above 150 K for all crystallographic directions. We ignored the temperature-independent contribution to the total susceptibility as it is very small compared with the raw data. The effective magnetic moment per formula unit $\mu_{\rm eff}$/fu is found to be equal to 18.87, 18.98 and 19.25 $\mu_{\rm B}$ for ***a***-, ***b***- and ***c***-axes, respectively. Assuming that the Co magnetic moment is zero, the effective magnetic moment per Ho ion is estimated as follows: $(\mu_{\rm eff}^{\rm Ho})^a = 10.89\ \mu_{\rm B}$, $(\mu_{\rm eff}^{\rm Ho})^b = 10.96\ \mu_{\rm B}$, $(\mu_{\rm eff}^{\rm Ho})^c = 11.11\ \mu_{\rm B}$. The anisotropy of the effective magnetic moment in Ho_3Co may be attributed to the low measuring temperatures in comparison

with the total splitting of the energy levels of Ho^{3+} in the strong crystal electric field. The values of $\mu_{\rm eff}^{\rm Ho}$ obtained along the main axes of Ho_3Co exceed the calculated effective magnetic moment $(\mu_{\rm eff}^{\rm Ho})^{\rm calc}$ 10.61 $\mu_{\rm B}$ for the free Ho^{3+} ion. The enhancement of the effective magnetic moment per formula unit is estimated to be about $\Delta\mu_{\rm eff}/{\rm fu} = 0.5$–$0.88\ \mu_{\rm B}$. These data are in agreement with previous susceptibility measurements performed in [8], where $\Delta\mu_{\rm eff}/{\rm fu} = 0.77$–$0.96\ \mu_{\rm B}$ was obtained on a single-crystalline sample of Ho_3Co in the temperature interval 77–800 K. A significant value of $\Delta\mu_{\rm eff}/{\rm fu}$ up to 1.07 and 1.18 $\mu_{\rm B}$ was also obtained for Gd_3Co and Dy_3Co [8], while in our recent study of an Er_3Co single crystal [14] we did not find any additional contribution to the value of $\mu_{\rm eff}/{\rm fu}$ in comparison with that calculated for the case when only Er ions have a magnetic moment. All these data suggest a dependence of $\Delta\mu_{\rm eff}/{\rm fu}$ on the type of the rare-earth ion in R_3Co compounds. A clear dependence of the extra contribution $\Delta\mu_{\rm eff}/{\rm fu}$ on the spin value of the R ion was observed for R_3Ni compounds [28]. Within the R_3Ni series with heavy rare earths the value of $\Delta\mu_{\rm eff}/{\rm fu}$ was found to decrease gradually from $\sim$1.1 $\mu_{\rm B}$ down to 0.47 $\mu_{\rm B}$ with increasing atomic number from Gd to Er, i.e. with decreasing spin value of the R ion. The reduction of $\Delta\mu_{\rm eff}/{\rm fu}$ from 0.55 to 0.02 $\mu_{\rm B}$ was also found for the R_3Rh family when going from R=Gd to R=Er (see [29] and references therein). Therefore, an additional contribution to the effective magnetic moment of R_3M seems to be an induced moment and may be associated with the particular M 3d-electrons. The value of $\mu_{\rm eff}$ per formula unit of R_3M may be presented as $\mu_{\rm eff} = \sqrt{3(\mu_{\rm eff}^{\rm R})^2 + (\mu_{\rm eff}^{\rm M})^2}$, where $\mu_{\rm eff}^{\rm R}$ and $\mu_{\rm eff}^{\rm M}$ are the effective magnetic moments associated with the rare earth and d-transition metal. The value of $\mu_{\rm eff}^{\rm M}$ may originate from spin fluctuations induced by the f–d exchange interaction in the d-electron subsystem of the M transition metal owing to the above-mentioned peculiarities of the crystal and electronic structure of these compounds. Using the value of $\mu_{\rm eff}/{\rm fu}$ obtained for Ho_3Co we estimated the value of $\mu_{\rm eff}^{\rm Co}$ that arises apparently from spin fluctuations produced by f–d exchange in the Co 3d-electron subsystem. According to this estimation the effective magnetic moment $\mu_{\rm eff}^{\rm Co}$ in Ho_3Co can be as large as about 4.3–5.7 $\mu_{\rm B}$, which exceeds the spin-only effective moment on Co^{2+}(3.87 $\mu_{\rm B}$).

As one can see in figure 2, the paramagnetic Curie temperature ϑ for Ho_3Co is anisotropic. The values of ϑ are obtained as $\vartheta_a = 28.8$ K, $\vartheta_b = 22.4$ K, $\vartheta_c = 28.4$ K for the ***a***-, ***b***- and ***c***-axes, respectively. When the magnetic ions occupy a single crystallographic position in the crystal lattice the anisotropy of ϑ allows for determining the second-order crystal field parameters, B_2^0. In the case of R_3Co with two non-equivalent 4c and 8d positions for R ions, only an effective parameter of the second order may be estimated. Its value is rather small for Ho_3Co and does not reflect the local single-ion anisotropy in the positions with the different symmetry, presumably due to the opposite sign of the second-order crystal field parameters. It should be noted that, according to crystal field calculations for the isostructural Er_3Co compound, the parameter B_2^0 was indeed found to exhibit a different sign for the 4c and 8d positions [31].

3.2. Magnetization process and magnetoresistance

The field dependences of the magnetization measured along the main crystallographic directions at $T = 1.5$ K in pulse magnetic fields up to 42 T are shown in figure 3. The magnetization is presented per Ho ion, bearing in mind the absence of an ordered magnetic moment on Co atoms (see above). Figure 3 shows that the magnetic moment per Ho ion does not reach the theoretical value $\mu_{\rm Ho} = 10\ \mu_{\rm B}$ for the free Ho^{3+} ion along all main axes even at the maximal field of 42 T, which is indicative of the presence of a complex non-collinear magnetic structure and the high magnetic anisotropy of Ho_3Co. In a low-field region, the magnetization curves show a metamagnetic behaviour: an increase of the magnetic field up

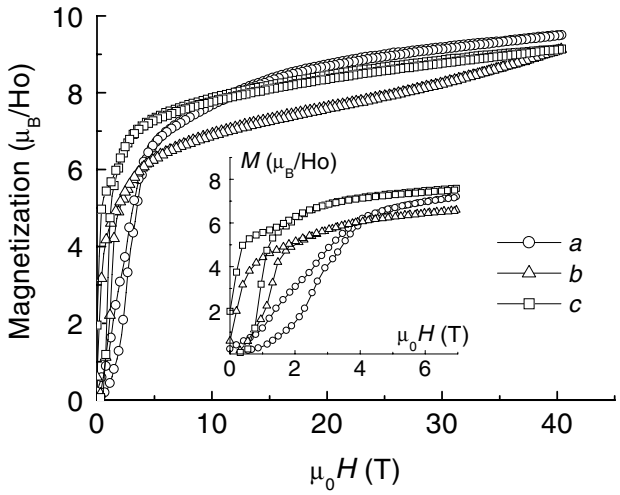

Figure 3. Magnetization of Ho_3Co measured in pulse fields along the main crystallographic directions at $T = 1.5$ K. The inset shows the low-field part of the field dependences.

to critical values leads to an abrupt increase of the magnetization. Such behaviour may be associated with the phase transitions of first-order nature from the initial AF_I state to the field-induced non-collinear ferromagnetic states (F_a, F_b and F_c) with resultant magnetizations along the ***a***-, ***b***- and ***c***-axes, respectively. It is to be noted that in some cases the field dependence of the magnetization obtained in pulse fields may strongly differ from that obtained in steady fields, especially, in the regions where the first-order phase transitions take place. In particular, such a difference was observed in the metamagnetic compounds Dy_3Co and $ErGa_2$ [32]. Therefore, in the present work for the detailed studies of the magnetization process in Ho_3Co we have also performed measurements of the magnetization in steady fields together with magnetoresistance measurements on the same samples, bearing in mind the very high sensitivity of the electrical resistivity to the change of the magnetic structure of metallic magnets.

Figures 4–6 display the field dependences of the magnetization and longitudinal magnetoresistance, measured along the main axes at $T = 4.2$ K on single crystals in steady fields starting from the ZFC state. The ***c***-axis of the Ho_3Co single crystal may be considered as an easy magnetization direction because the maximum value of the magnetization is reached along this direction with the application of a small magnetic field (see figure 3). However, each Ho ion at the two crystallographic sites in the magnetic unit cell of Ho_3Co is expected to have its own magnetic easy axis because of the inequivalent crystallographic sites and thus different low-lying CEF states. Apparently the shape of the field dependence of the magnetization obtained along the ***c***-axis (figure 4(a)) seems to be quite typical for ferromagnetic materials, which contradicts the neutron diffraction data. On the other hand, it should be noted that in many cases the magnetization measurements alone and, particularly, the shape of the magnetization curve, do not allow one to distinguish a high-anisotropic ferromagnet from a metamagnetic compound (see [33]). In the case of Ho_3Co a new anomaly was observed, which differs from the magnetization process of the ordinary high-anisotropic ferromagnets. As can be seen from the inset in figure 4(a), the initial magnetization curve lies outside the hysteresis loop. We have also found a big difference between the magnetization process along the ***c***-axis of Ho_3Co and the high-anisotropic ferromagnets by measurements of the longitudinal magnetoresistance. In fact, an application of a magnetic field along the ***c***-axis leads to an

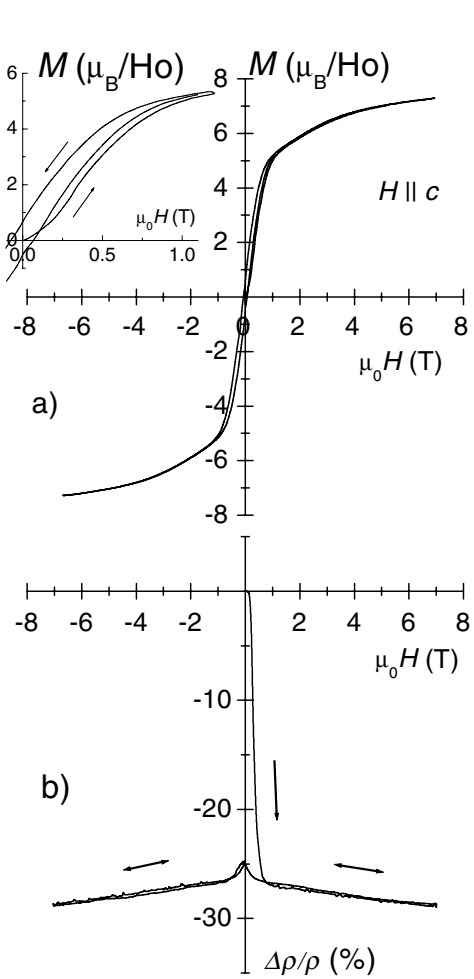

Figure 4. Field dependences of the magnetization (a) and longitudinal magnetoresistance (b) measured along the ***c***-axis at $T = 4.2$ K. The inset shows a low-field part of the $M(H)$ dependence in detail.

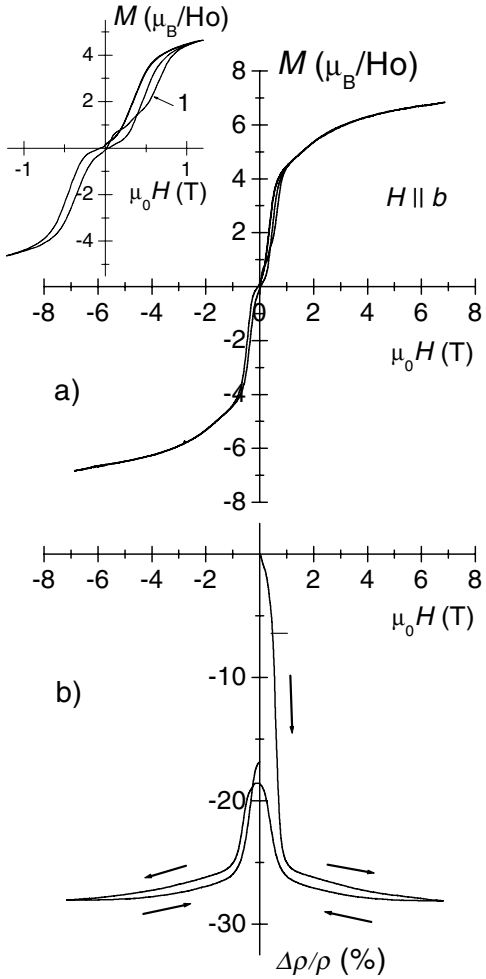

Figure 5. Field dependences of the magnetization (a) and longitudinal magnetoresistance (b) measured along the ***b***-axis at $T = 4.2$ K. The inset shows a low-field part of the $M(H)$ dependence in detail.

abrupt decrease (down to -29%) of the electrical resistivity of the single crystal (shown in figure 4(b)). It should be noted that the giant magnetoresistance (GMR) ($|\Delta\rho/\rho| \sim 30$–$50\%$), which accompanies the field-induced magnetic phase transitions, was earlier observed in isostructural antiferromagnetic compounds Gd_3Co [9] and Dy_3Co [13, 18], while Tb_3Co, having a non-collinear ferromagnetic structure, was found to reveal a significantly smaller change of the electrical resistivity ($\sim$3–5%) under application of a magnetic field along the easy ***c***-axis [7, 12]. The GMR effect in the antiferromagnetically ordered compounds R_3Co was previously attributed to the change of their electronic structure, which is likely to be caused by the disappearance of superzones and the energy gap on superzone boundaries at the transformation of the initial antiferromagnetic structure to the field-induced ferromagnetic state [34, 35]. This conclusion was further supported by the significant change of the electronic specific heat at the AF–F transitions in these compounds [9, 13, 35]. Because

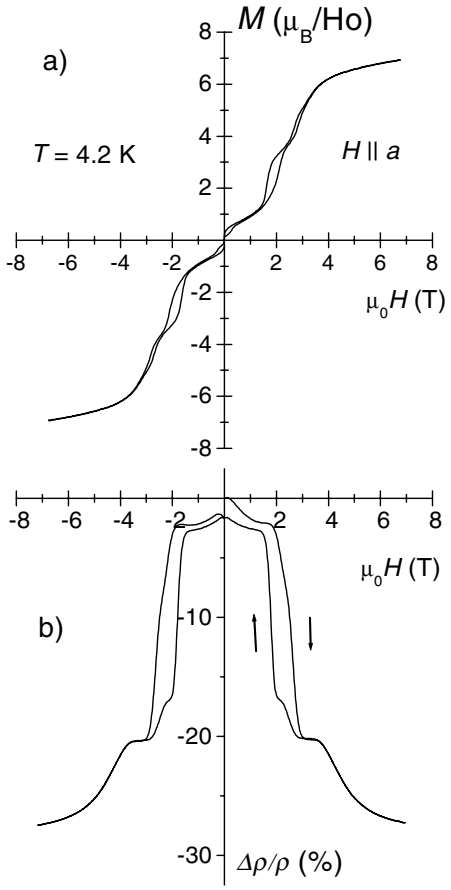

Figure 6. Field dependences of the magnetization (a) and longitudinal magnetoresistance (b) measured along the ***a***-axis at $T = 4.2$ K.

of the presence of the incommensurate AF structure in Ho_3Co (see above) one may conclude that the GMR observed along the ***c***-axis in this compound originates from superzone effects as well. Surprisingly, the giant reduction of the resistivity under application of a small magnetic field (∼0.8 T) is found to be irreversible. As it follows from figure 4(b), switching off the field does not restore the initial value of the resistivity. In the following magnetization cycles the magnetoresistance varies by a few per cent (from −29% to −25%) when the external field changes within the range $-7\ \mathrm{T} < \mu_0 H < 7\ \mathrm{T}$. These data allow us to suggest that the Ho_3Co single crystal undergoes a field-induced phase transition of the first-order nature along the ***c***-axis from the initial AF_I state to the non-collinear F_c state, which is metastable. The magnetization reversal of the sample in the induced F_c phase is accompanied by an ordinary magnetoresistance effect of about 4%. In fact, the sample may be reinstated into the initial AF_I phase by heating it above 8 K (see below). The metastable ferromagnetic state, which can be produced in an antiferromagnetically ordered compound by application of a magnetic field, was also found in the isostructural compounds Dy_3Co [13, 18] and $(Tb_{1-x}Y_x)_3Co$ at $x \geqslant 0.3$ [7].

The field dependences of both the magnetization and magnetoresistance measured along the ***b***-axis (figure 5) indicate that the magnetization reversal in this field direction is a more

complicated process than that suggested by the magnetization measurements alone. As can be seen from the inset in figure 5, the initial magnetization curve exhibits a jump at a higher critical field than that at the second magnetization cycle. Considering the magnetoresistance data presented in figure 5(b), the first magnetization jump along the ***b***-axis may be associated with the phase transition from the initial AF_I state to the non-collinear ferromagnetic structure (F_b) with the resultant magnetization parallel to the field direction. However, this AF_I–F_b transition also seems to be irreversible since the large remnant magnetoresistance ($\sim -17\%$) is observed after switching off the field, although the remnant magnetization along this axis is nearly zero. The magnetic state characterized by such a remnant magnetoresistance may be associated with a new metastable antiferromagnetic phase AF_b, which appears after application of a field along the ***b***-axis in the first magnetization cycle. The change of the magnetization during the subsequent cycles involves the field-induced AF_b–F_b transition, which is accompanied by a significant change of the $\Delta\rho/\rho$ value between -17% and -28% (figure 5(b)).

Figure 6 displays the field dependences of the magnetization and longitudinal magnetoresistance measured along the ***a***-axis at 4.2 K. The distinctive features of the magnetization process along this axis are the presence of a small ferromagnetic component ($\sim 0.4\ \mu_B$) which is clearly seen in the low-field region and two steps on the magnetization curve at higher fields. The metamagnetic transitions at critical fields ~ 2 and ~ 2.8 T are also accompanied by a magnetoresistance effect of different value. Such a difference in $\Delta\rho/\rho$ at each transition may arise from the different change of the Fermi surface and the group velocity [34]. The remnant magnetoresistance after a full cycle of the reversal magnetization is rather small for this field direction ($\sim 1.5\%$). The ferromagnetic component is found to exist at $H \parallel \boldsymbol{a}$ only in the low-temperature phase, i.e. below T_t, as can be seen from figure 7(a), which presents the field dependences of the magnetization measured at different temperatures.

Based on the critical transition fields of the metamagnetic transitions as well as the irreversibility of some transitions observed in Ho_3Co, we suggest that this compound exhibits a set of magnetic structures which are very close to each other in respect to their free energy despite the strong magnetocrystalline anisotropy of this compound. The field-induced transition between different spin configurations in Ho_3Co is suggested to proceed via spin flip processes of magnetic moments along their individual easy axes. It should be noted that multi-step magnetic transitions are observed in a number of rare-earth compounds having incommensurate magnetic structures [36]. When the R ion is of non-Kramers type such as Ho^{3+}, the ground state may be non-magnetic because of CEF splitting of the multiplet. The magnetic moment on Ho ions results in this case from exchange interactions, which mix the wave functions of the CEF levels. This frequently leads to the appearance of an amplitude-modulated structure at $T < T_N$. Compounds having an incommensurate structure just below T_N in most cases exhibit a phase transition (one or more) with decreasing temperature to magnetic structures with another periodicity, generally with a shorter period [37]. This situation apparently exists in Ho_3Co when the temperature decreases below $T_t = 8$ K. The appearance of the small ferromagnetic component at $T < T_t$ along the ***a***-axis may be considered as evidence of the unbalanced character of the low-temperature magnetic structure, while the AF_{II} incommensurate structure, which is observed at $T_t < T < T_N$, exhibits a full compensation of the up and down magnetic moments. The last follows from the field dependences of the magnetization measured along the main crystallographic directions at $T = 15$ K (figure 7(b)). The magnetization curves presented in figure 7(b) do not reveal any indication of the presence of a ferromagnetic component at this temperature along the main crystallographic directions. When the magnetic field is applied along the ***c***-axis, the magnetization curve exhibits a sharp increase of the magnetization at ~ 0.3 T which may be associated with the phase transition from the AF_{II} structure to the field-induced F state with projection of the magnetization onto the

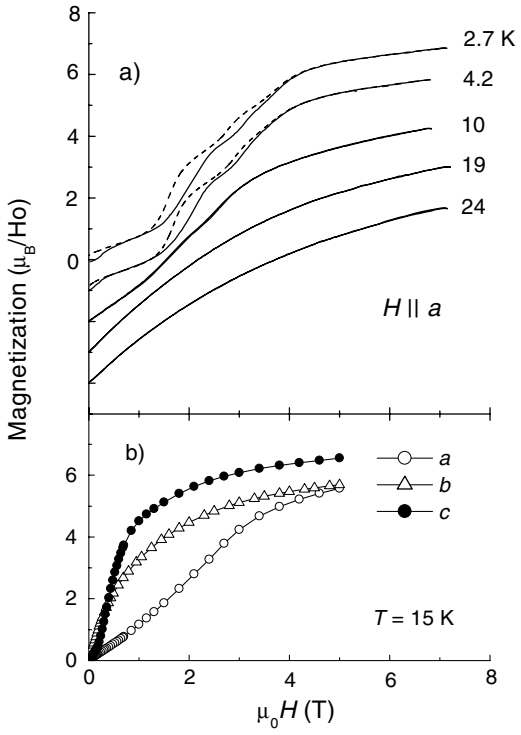

Figure 7. (a) Field dependences of the magnetization of Ho_3Co measured along the ***a***-axis at various temperatures and (b) field dependences of the magnetization measured along ***a***-, ***b***- and ***c***-axes at $T = 15$ K.

field direction. The positive curvature of the magnetization curve along the ***a***-axis may also be indicative of the phase transition at a critical field around 2.5 T. These transitions are smoothed because of the increased temperature. The emergence of a small ferromagnetic component with squaring up of the incommensurate structure with decreasing temperature was observed in $PrGa_2$ compound [38]. As was shown in [38] by magnetization and neutron diffraction measurements, a net ferromagnetic component appears in $PrGa_2$ through the growing of higher harmonics of the propagation vector of the incommensurately modulated structure with decreasing temperature. According to the neutron diffraction study of a Ho_3Co single crystal [20], an analogous behaviour, i.e. the growth of higher harmonics of $\boldsymbol{k}_2$, is observed in this compound below T_t as well.

3.3. Electrical resistivity

The temperature dependences of the electrical resistivity measured along the main crystallographic axes of Ho_3Co are presented in figure 8(a). The values of the residual resistivity of Ho_3Co seem to be high compared with values for other R_3M (see [7–9]). Another common feature is a pronounced convexity of $\rho(T)$ curves and tendency to saturation of the resistivity with increasing temperature. In the low temperature range the $\rho(T)$ dependences measured for samples cooled at zero magnetic field reveal anomalies caused by the antiferromagnetic ordering of the Ho magnetic moments below T_N and by the spontaneous transformation of the magnetic structure at $T = T_t$. As one can see in the inset of figure 8(a),

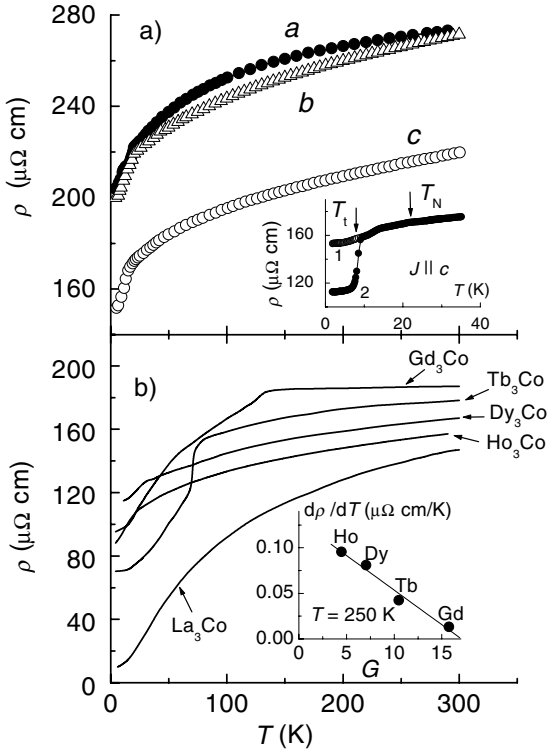

Figure 8. (a) Temperature dependences of the electrical resistivity measured along the ***a***-, ***b***- and ***c***-axes of Ho_3Co single crystals. The inset shows the low-temperature part of the $\rho(T)$ dependence measured at $H = 0$ along the ***c***-axis on the sample cooled down at different conditions: curve 1 corresponds to the ZFC regime; curve 2 was obtained for the sample cooled down at $\mu_0 H = 2$ T. (b) The averaged temperature dependences of the electrical resistivity for R_3Co (R = Gd, Tb, Dy, Ho). The $\rho(T)$ curves are arranged in order of increasing atomic number of the R ion from Gd to Ho. Inset: the $d\rho/dT$ versus G dependence taken at $T = 250$ K.

which displays the $\rho(T)$ dependence along the ***c***-axis below 40 K, these anomalies are somewhat smoothed (see curve 1). Since the Ho_3Co compound exhibits AF order at $T < T_N$, its electrical resistivity can be expressed as [34]

$$\rho(T) = \frac{\rho_0 + \rho_{ph}(T) + \rho_{mag}(T)}{1 - \delta}, \tag{1}$$

where ρ_0, $\rho_{ph}(T)$, $\rho_{mag}(T)$ are the residual, phonon and magnetic contributions respectively; $\delta = \Gamma m$ is proportional to the width of the energy gap at the new zone boundaries that appeared in the AF state, m is the normalized magnetization, Γ depends on the exchange integral between the conduction electrons and f-electrons of the R ions and includes the contributions from all new superzone boundaries which cut the Fermi surface. The magnetic contribution $\rho_{mag}(T)$ is expected to arise from the scattering of conduction electrons by localized 4f-electrons of Ho and spin fluctuations in the d-electron subsystem. The change of the δ-value owing to the transformation of the magnetic structure of Ho_3Co with temperature or/and under application of magnetic field may result in an appreciable change of $\rho(T)$. It can be clearly seen from the inset in figure 8(a) that there appears to be a pronounced difference between the resistivity measured with increasing temperature at zero external field for the sample cooled down to $T = 2$ K at zero external field (curve 1) and at $\mu_0 H = 2$ T (curve 2). After cooling down and

switching off the field the sample being in the field-induced F_c state shows a significantly lower resistivity ($\Delta\rho/\rho \approx -26.5\%$) at $T = 2$ K, which increases abruptly when the temperature reaches $T_t = 8$ K. Above this temperature both curves 1 and 2 become almost identical. Since at $T < T_t$ the field-induced $AF_I \rightarrow F_c$ transition is of the first order, one can suggest that the change of the magnetic state from the metastable F_c phase to the AF_{II} phase with increasing temperature above 8 K also occurs through a phase transition of the first order, i.e. via formation of the AF_{II} nucleus and their avalanche-like growth within the F_c matrix owing to the thermal activation. It should be noted that the change of the electrical resistivity at the $F_c \rightarrow AF_{II}$ transition may also be influenced by the variation of the magnetic contribution ρ_{mag} in the expression (1) owing to the possible difference in the spin wave dispersion in the subsystem of localized 4f moments and s-electron scattering on the quadrupolar moment of the 4f-electron shell of Ho ions in the F_c and AF_{II} phases.

The anisotropic behaviour of $\rho(T)$ for Ho_3Co in the paramagnetic region (figure 8(a)) may have magnetic and non-magnetic origins. Since the Ho ion has non-zero orbital momentum, the anisotropy of the electrical resistivity of Ho_3Co above T_N can be ascribed to anisotropy of the s-electron scattering by quadrupolar moment of 4f-electron shell of Ho ions. As is shown in [39], such a mechanism contributes significantly to the anisotropy of ρ for pure rare earths above their ordering temperatures. However, it should be noted that substantial anisotropy of the electrical resistivity was also observed for La_3Co [40] where La has an empty 4f-shell and in Gd_3Co [9] where the Gd ion is in the S-state. Therefore, one can attribute the anisotropy of the resistivity in Ho_3Co above T_N primarily to the anisotropy of the effective mass of conduction electrons.

The saturation of the resistivity with increasing temperature in the paramagnetic region in f–d intermetallics may result from several mechanisms [41]: (i) the s–d scattering which is temperature dependent owing to the temperature dependence of the DOS value and its derivatives; (ii) the influence of spin fluctuations in the d-electron subsystem; (iii) the effect of the crystalline electric field and (iv) short-range magnetic correlations above the ordering temperature. In order to exclude the anisotropy of the electrical resistivity of Ho_3Co when analysing the saturation effect we have averaged the resistivities using the following formula: $\rho(T) = 1/3[\rho_a(T) + \rho_b(T) + \rho_c(T)]$, where $\rho_i(T)$ is the temperature dependence of the resistivity measured along the ith direction on single-crystalline samples. The averaged $\rho(T)$ curve for Ho_3Co is shown in figure 8(b) together with analogous curves for other R_3Co compounds with heavy rare earths (R = Gd, Tb, Dy [15]), which are displayed for comparison. The $\rho(T)$ curves presented in figure 8(b) are shifted relatively to the $\rho(T)$ dependence for Gd_3Co and arranged in order of increasing atomic number of the R ion from Gd to Ho. Unfortunately, we did not find the resistivity data for all three axes of Er_3Co in the literature. For the paramagnetic compounds, we plotted in figure 8(b) the resistivity data of the single crystal La_3Co taken from [40]. Since the $\rho(T)$ dependence of La_3Co as well as of other paramagnetic compounds (Y_3Co [7, 8], Y_3Ni [28],) also demonstrate a tendency towards saturation with increasing temperature one can suggest that such behaviour does not directly relate to the 4f-electrons of R ions. It should be noted that the electrical resistivity is found to saturate in many compounds, the physical properties of which are strongly influenced by spin fluctuations. Among the f–d intermetallics, well-known spin fluctuating systems are the Laves phases RCo_2 [41]. Nevertheless, besides the saturation effect of the resistivity such systems also reveal a significantly enhanced value of the electronic specific heat coefficient γ. As for the γ-value for paramagnetic R_3M compounds, it seems to be typical for metallic systems without significant influence of spin fluctuations: 14 for Y_3Ni [14]; 15 for Y_3Co [21]; 11 for Y_3Rh [22], 25 for La_3Co [40] and 20.6 for La_3Ni [42] (all data are given in mJ mol^{-1} K^{-2}). When divided by the number of ions in the formula unit, the values of γ for these compounds seem to be

comparable with those for pure metals (for Y, La, Co and Ni see for example [43]). The enhancement of γ in La_3Co and La_3Ni results apparently from the enhanced electron–phonon interaction since this compound exhibits superconducting properties below 4.5 K [40, 42]. Therefore, the negative curvature of $\rho(T)$ dependences observed for paramagnetic R_3M can scarcely be attributed to spin fluctuations. In our opinion, such behaviour of $\rho(T)$ for R_3M (R = Y, La) may be mainly associated with the influence of the s–d scattering mechanism because of the significantly narrower d-band in R_3M (1.0–1.7 eV) than in pure d-metals (5–6 eV) (see [26]).

As can be seen from figure 8(b), the slope of the $\rho(T)$ curves for R_3Co with R = Gd, Tb, Dy and Ho above 150 K, where all compounds exhibit paramagnetic behaviour, varies significantly for different R ions. Nevertheless, we can assume that the phonon and s–d scattering contributions to the total resistivity change in this temperature interval are nearly the same because of the identical crystal and electronic structures. As for the phonon contribution $\rho_{ph}(T)$, its similarity for the compounds with R = Gd, Tb, Dy and Ho results from the proximity of their Debye temperatures: the values of Θ_D lie between 157 K for Gd_3Co [9] and 153 K for Ho_3Co (see below). In respect of the magnetic contribution to the total resistivity caused by s-electron scattering by localized magnetic moments of R ions, it is well known [44] that such a contribution should be temperature independent in the paramagnetic region neglecting the influence of short-range order correlations above the ordering temperature:

$$\rho_{s-f} \propto (A_{sf})^2(g-1)^2 J(J+1). \tag{2}$$

Here $G = (g-1)^2 J(J+1)$ is the de Gennes factor and A_{sf} is the s–f exchange integral. In Ho_3Co such a contribution should be lower than that in Gd_3Co owing to the lower spin value. The presence of the temperature-independent magnetic contribution above the ordering temperature was indeed observed in pure rare earths and their alloys as well as in many rare-earth intermetallic compounds with non-magnetic partners [45]. However, analysis of the specific heat data for Gd_3Co [21] has shown that the magnetic contribution to the total specific heat of this compound persists over a wide temperature range above T_N, which implies the presence of short-range f–f magnetic correlations. One can therefore assume that such kind of correlations also exist in Ho_3Co. In order to examine this additional contribution in the temperature scale, we measured the electrical resistivity of the Ho_3Co single crystal together with Gd_3Co and Y_3Co for the current $j \parallel c$ at temperatures up to 600 K (see figure 9). The paramagnetic compound Y_3Co can be considered as a reference material above 170 K. Below this temperature Y_3Co exhibits some anomalies in the electrical resistivity [8, 21] which are probably associated with the changes of the crystal structure. The temperature variation of the additional magnetic contribution to the resistivity of Ho_3Co and Gd_3Co above 170 K may be obtained with the following formula:

$$\Delta\rho(T) = \rho(T)_{R_3Co} - [\rho(T) - \rho_0(T)]_{Y_3Co} = \rho_{s-f} + \Delta\rho_{add}(T). \tag{3}$$

Assuming that the s–d scattering is nearly the same for all R_3Co with heavy rare earths and the ρ_{s-f} contribution is temperature independent according to (2), the behaviour of $\Delta\rho(T)$ in the paramagnetic region may be attributed mainly to $\Delta\rho_{add}(T)$. As can be seen in figure 9, the most pronounced growth of $\Delta\rho(T)$ with decreasing temperature from 600 K is observed for Gd_3Co having a larger spin value. An analogous subtraction procedure performed for pure rare earths as well as for rare-earth compounds with non-magnetic partners [41, 44] has revealed much smaller anomalies above their magnetic ordering temperatures. In the case of Gd metal the inelastic neutron scattering experiments performed on a single crystal of ^{160}Gd have revealed the presence of spin pair correlations even at 850 K [45]; however, these spin pair correlations at high temperatures and short-range correlations, which appear in Gd with

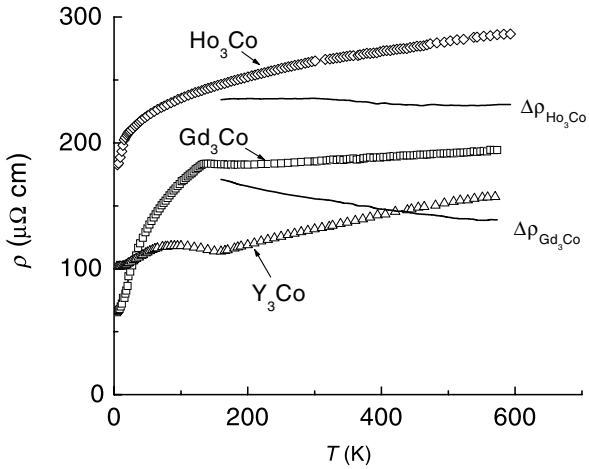

Figure 9. The $\rho(T)$ dependences measured for R_3Co (R = Gd, Ho, Y) along the ***c***-axis up to 600 K. Solid lines demonstrate $\Delta\rho(T)$ dependences according to (3) for Gd_3Co and Ho_3Co.

decreasing temperature approaching T_C, do not result [46] in the extra contribution in such a wide temperature range as in Gd_3Co. It should be noted that the influence of short-range magnetic correlations on the electrical resistivity above the magnetic ordering temperature according to most existing theories is restricted within a narrow temperature interval (see [47]), while in our case the additional magnetic contribution $\Delta\rho$ extends over 3–5 times T_N, which cannot be described by the aforementioned conventional theories. In our opinion, the presence of the significant $\Delta\rho_{add}(T)$ contribution to the electrical resistivity of R_3M observed in a wide temperature range above the magnetic ordering temperature cannot be explained by short-range f–f correlations alone without taking into account the conduction electron scattering on spin fluctuations due to the f–d-exchange in the d-electron subsystem (see above). We consider such induced spin fluctuations as a main origin of the additional contribution to the conduction electron scattering observed above the ordering temperatures in R_3M. The value of $\Delta\rho_{add}$ and its temperature extension should be dependent on the local amplitude of spin fluctuations in the 3d-electron subsystem and therefore on the spin value of the R ion which produces such fluctuations. This assumption is confirmed by the pronounced dependence of the value of $d\rho/dT$ taken at $T = 250$ K (i.e. well above the ordering temperature of R_3Co) on the de Gennes factor $G = (g-1)^2 J(J+1)$ (see the inset in figure 8(b)).

3.4. Heat capacity

The temperature dependence of the specific heat measured on a single-crystalline sample Ho_3Co is presented in figure 10(a). The $C_p(T)$ dependence exhibits a pronounced maximum at ~20 K, i.e. below the Néel temperature $T_N = 22$ K, and an upturn at $T < 4$ K. The presence of a maximum of the specific heat below the ordering temperature is a characteristic feature of magnetic systems exhibiting amplitude-modulated structures [48]. The low-temperature upturn of C_p in figure 10(a) is associated with the nuclear contribution C_n that arises from the huge hyperfine interaction of the Ho nucleus having the spin value $I = 7/2$ with the effective field of about 900 T [49]. As it follows from inset in figure 10(a), only a smeared anomaly is observed around the critical temperature T_t. In figure 10(b) we plotted the magnetic contribution $C_m(T)$ to the total specific heat which was obtained after subtracting off the nuclear, electronic and lattice contributions: $C_m(T) = C_p(T) - C_n(T) - C_{el}(T) - C_{latt}(T)$.

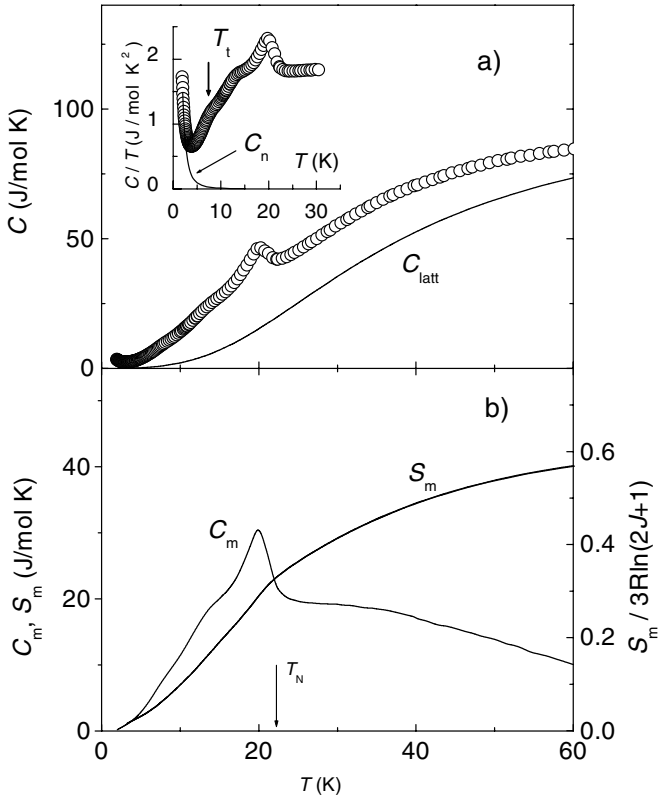

Figure 10. Temperature dependence of the specific heat for the Ho_3Co single crystal: (a) experiment (open circles) and the lattice contribution $C_{\rm latt}$ calculated with $\Theta_{\rm D} = 153$ K, (b) magnetic contribution to the specific heat and magnetic part of the entropy. The inset shows the C_p/T versus T dependence in a low-temperature region. The solid line corresponds to the nuclear contribution $C_{\rm n}$.

The temperature dependence of the nuclear contribution to the specific heat of Ho_3Co at $T > 2$ K was calculated using data for the pure Ho metal [49] to the first approximation as $C_{\rm n}(T) = \alpha\ T^{-2}$, where α is a constant. The results of this calculation are shown in the inset of figure 10(a). For the electronic contribution $C_{\rm el}(T) = \gamma T$ we have taken the γ value of 15 mJ mol^{-1} K^{-2}, which was obtained for the paramagnetic isostructural compound Y_3Co [21]. As mentioned above, the Gd_3M compounds (M = Co, Ni, Rh) are found to reveal a significantly enhanced T-linear specific heat, apparently because of the huge contribution from spin fluctuations, which are induced in the d-electron subsystem by the exchange interaction acting from f-electrons of Gd ions. Unfortunately, we did not succeed in unambiguously evaluating γ for Ho_3Co from our measurements owing to the large nuclear and magnetic contributions to $C_p(T)$ in low-temperature range. As for the lattice contribution $C_{\rm latt}(T)$, which is shown in figure 10(a) by the solid line, it was calculated using a simple Debye model with the Debye temperature $\Theta_{\rm D} = 153$ K. This value was obtained using the Debye temperature $\Theta_{\rm D} = 157$ K for Gd_3Co [9] and taking into account the difference in atom masses of Gd and Ho. The value of $\Theta_{\rm D}$ for Gd_3Co was obtained in [9] by sound velocity and thermal expansion measurements. As it follows from figure 10(b), the $C_{\rm m}(T)$ dependence extends for temperatures above $3T_{\rm N}$, and it exhibits not only a maximum just below the Néel temperature

$\sim$22 K associated with the long-range magnetic order due to the RKKY exchange interaction, but it also shows a broad hump which can be mainly attributed to the Schottky-type heat capacity from the crystal field effects (C_{cf}). Thus, the magnetic heat capacity of Ho_3Co is suggested to include two contributions: $C_m = C_{exch} + C_{cf}$. The significant part of C_{exch} in Ho_3Co apparently persists above T_N owing to the retention of short-range correlations between Ho magnetic moments. As mentioned above, the presence of such correlations between the local 4f moments was derived from specific heat measurements for Gd_3Co and Gd_3Rh compounds in which the Gd ion has zero orbital moment [21, 22].

By integrating $C_m(T)/T$ we have calculated the magnetic entropy of Ho_3Co which is plotted in figure 10(b). The maximal value of the magnetic entropy $S_m = 3\ R\ln(2J+1) = 70.7$ J mol^{-1} K^{-1} for Ho_3Co should be observed when all the energy levels of the multiplet are populated. As it follows from figure 10(b), at $T = 60$ K the value of S_m is significantly lower than the maximum theoretical value, which implies a large crystal field splitting of the ground state multiplet of the Ho^{3+} ion in this compound. According to [29] the magnetic entropy of Ho_3Co does not reach the theoretical value even at $T = 300$ K. These data are supported by the above-discussed anisotropy of the Ho effective magnetic moment measured along the main axes. Since the magnetic entropy at the Néel temperature $T_N = 22$ K reaches a value about 23.4 J mol^{-1} K^{-1} $\approx 3\ R\ln(2.56)$, one can suggest that the ground state of Ho ions in this compound is a quasi-doublet and the second excited state is also admixed below T_N.

4. Summary

The investigation of the magnetic state and physical properties of Ho_3Co single crystals shows that this compound exhibits all main features which are common to the R_3M family. The magnetization measurements along the main crystallographic directions in steady and pulse fields together with the previous neutron diffraction study have revealed a complex antiferromagnetic arrangement of Ho magnetic moments which appears below $T_N = 22$ K. Further decrease of the temperature below $T_t \approx 8$ K leads to a phase transition from the incommensurate structure AF_{II} to another structure AF_I, which is characterized by the higher harmonics of the wavevector $\boldsymbol{k}_2 = (0.15\ 0\ 0)$ and by the presence of a small ferromagnetic component along the $\boldsymbol{a}$-axis. These magnetic structures are suggested to arise from the non-Kramers Ho^{3+} ions in combination with competition between the RKKY exchange interaction and the low-symmetry crystal electric field. The anisotropy of the effective magnetic moment and paramagnetic Curie temperature derived from magnetic susceptibility measurements of Ho_3Co as well as the large Schottky-type contribution to the total specific heat, which extends over a wide temperature interval above T_N, are indicative of the strong influence of the crystal electric field on the energy level scheme of the Ho^{3+} ion. Specific heat data allow us to suggest that this ground state of Ho^{3+} in the Ho_3Co compound is a quasi-doublet.

Despite the absence of an ordered magnetic moment on the Co atoms in Ho_3Co as in other R_3Co, the Co 3d-electron subsystem significantly affects the physical properties of these compounds. The effective magnetic moment per formula unit, μ_{eff}/fu, of Ho_3Co is found to exceed the value calculated for free Ho ions and a non-magnetic Co sublattice. The enhancement of the effective magnetic moment is thus ascribed to the presence of an additional contribution, μ_{eff}^{Co}, which may result from spin fluctuations induced by the f–d exchange in the 3d-electron subsystem of Co. The local amplitude of the spin fluctuations and its temperature variation and, consequently, the value of μ_{eff}^{Co}, should depend on the spin value of the R ion. The value of μ_{eff}^{Co} is estimated to be about 4.3–5.7 μ_B for Ho_3Co. An induced nature of μ_{eff}^{Co} is clearly evidenced by the presence of the pronounced dependence of the extra contribution $\Delta\mu_{eff}$/fu on the type of R ion, as is observed for different R_3M compounds (see [8, 14, 28, 29]).

Because of the complex non-collinear magnetic structure, which appears in Ho_3Co below T_N, the field-induced phase transitions are found to occur under application of an external magnetic field applied along the main axes of the single crystal. Using magnetoresistance measurements as a sensitive indicator of the magnetic structure transformations, an irreversibility of the phase transitions under application of magnetic field has been revealed along the ***c***- and ***b***-axes below T_t. These data together with low values of critical transition fields imply that several magnetic structures of Ho_3Co are very close to each other with respect to their free energy. The significant magnetoresistance effect ($\sim -30\%$) which accompanies the field-induced phase transitions in Ho_3Co is associated with superzone effects as in other antiferromagnetically ordered compounds R_3Co. The measurements of electrical resistivity of Ho_3Co performed in the temperature range up to 600 K have revealed that this compound exhibits another temperature coefficient of the electrical resistivity above its magnetic ordering temperature compared with that observed for other R_3Co. The temperature dependence of the electrical resistivity of Ho_3Co as well as other R_3M compounds in the paramagnetic regime, we suggest, is mainly determined by the competition of two contributions. The first one results from the s–d scattering which causes a growth of the resistivity with the temperature and the negative curvature of the $\rho(T)$ dependence. The second contribution, which decreases with increasing temperature, is due to the scattering of conduction electrons by spin fluctuations induced through f–d exchange in the d-electron subsystem of the transition metal. Bearing in mind that the s–d scattering contribution does not vary significantly for different R_3Co compounds with heavy rare earth, the change of the temperature coefficient of the resistivity with increasing atomic number of R ion starting from Gd is, we think, controlled mainly by the scattering by spin fluctuations in the 3d-electron subsystem of Co, since the local amplitude of these spin fluctuations owing to their induced character is suggested to depend on the spin value of the R ion. The maximum value of this spin fluctuation contribution and its large temperature extension in the case of Gd_3M (M = Ni, Co, Rh) owing to the maximal spin value of Gd results in the nearly zero value of the temperature coefficient of the resistivity of these compounds in a wide temperature range ($\sim$140–400 K), while the reduction of this additional contribution with decreasing the spin value of the R ion in R_3M leads to a growth of $d\rho/dT$, as is evidenced by the measurements of $\rho(T)$ dependences for different R_3M. These results emphasize the significant influence of the transition metal in R–M intermetallics on their physical properties even in the case where the M atoms do not possess an own magnetic moment.

Acknowledgments

This work was supported in part by the Russian Foundation for Basic Research (Grant No. 04-02-96060). One of us (JGP) acknowledges financial support of the CSCMR at Seoul National University and the CNRF project.

References

[1] Cromer D T and Larson A C 1961 *Acta Crystallogr.* **14** 1226
[2] Buschow K H J and van der Goot A S 1969 *Less Common Met.* **18** 309
[3] Feron J-L, Gignoux D, Lemaire R and Paccard D 1970 *Less Elements des Terres Rares* **2** 75
[4] Primavesi G J and Taylor K N R 1972 *J. Phys. F: Met. Phys.* **2** 761
[5] Deryagin A V, Baranov N V and Reimer V A 1977 *Zh. Exp. Teor. Fiz.* **73** 1389
Deryagin A V, Baranov N V and Reimer V A 1977 *Sov. Phys.—JETP* **46** 731 (Engl. Transl.)
[6] Deryagin A V and Baranov N V 1980 *Fiz. Met. Metall.* **49** 1245

[7] Baranov N V, Deryagin A V, Kozlov A I and Sinitsyn E V 1986 *Fiz. Met. Metallo.* **61** 733
Baranov N V, Deryagin A V, Kozlov A I and Sinitsyn E V 1986 *Phys. Met. Metallogr.* **61** 97 (Engl. Transl.)
[8] Talik E, Szade J, Neumann J, Winiarska A, Winyarski A and Chelkowski A 1988 *J. Less-Common Met.* **138** 129
[9] Baranov N V, Andreev A V, Kozlov A I, Kvashnin G M, Nakotte H, Aruga Katori H and Goto T 1993 *J. Alloys Compounds* **202** 215
[10] Lu Q F, Umehara I, Adachi Y, Endo M and Sato K 1997 *J. Phys. Soc. Japan* **66** 1480
[11] Umehara I, Lu Y, Lu Q F, Adachi Y, Endo M, Sato K, Bartashevich M and Goto T 1998 *J. Appl. Phys.* **83** 6961
[12] Baranov N V, Markin P E, Nakotte H and Lacerda A 1998 *J. Magn. Magn. Mater.* **177–181** 1133
[13] Baranov N V, Bauer E, Hauser R, Calatanu A, Aoki Y and Sato H 2000 *Eur. Phys. J.* B **16** 67
[14] Baranov N V, Hilscher G, Korolev A V, Markin P E, Michor H and Yermakov A A 2002 *Physica* B **324** 179
[15] Baranov N V, Hilscher G, Markin P E, Michor H and Yermakov A A 2004 *J. Magn. Magn. Mater.* **272–276** 637
[16] Gignoux D, Lemaire R and Paccard D 1970 *Solid State Commun.* **8** 391
[17] Gignoux D and Lemaire R 1974 *ICM-73: Proc. Int. Conf. on Magn. (Moscow, Aug. 1973)* vol 5, p 361
[18] Baranov N V, Pirogov A N and Teplykh A E 1995 *J. Alloys Compounds* **226** 70
[19] Adachi Y, Lu Y, Umehara I, Sato K, Ohashi M, Ohoyama K and Yamaguchi Y 1999 *J. Appl. Phys.* **85** 4750
[20] Podlesnyak A, Daoud-Aladine A, Zaharko O, Markin P and Baranov N 2004 *J. Magn. Magn. Mater.* **272–276** 565
[21] Baranov N V, Yermakov A A, Markin P E, Possokhov U M, Michor H, Weingartner B and Hilscher G 2001 *J. Alloys Compounds* **329** 22
[22] Baranov N V, Inoue K, Michor H, Hilscher G and Yermakov A A 2003 *J. Phys.: Condens. Matter* **15** 531–8
[23] Hilscher G, Michor H, Baranov N V, Markin P E and Yermakov A A 2003 *Acta Phys. Pol.* B **34** 1205
[24] Gratz E, Hilscher G, Michor H, Markosyan A, Talik E, Czizjek G and Mexner W 1996 *Chech. J. Phys.* **46** (Suppl. 4) 2031
[25] Tsang T-W Jr, Gschneidner K A, Schmidt F A and Thome D K 1985 *Phys. Rev.* B **31** 235
[26] Talik E and Neumann M 1994 *Physica* B **193** 207
Talik E, Neumann M, Slebarski A and Winiarski A 1995 *Physica* B **212** 25
Talik E and Neumann M 1995 *J. Magn. Magn. Mater.* **140–144** 795
[27] Duc N H 1997 *Handbook on the Physics and Chemistry of Rare Earths* vol 24, ed K A Gschneidner Jr and L Eyring (Amsterdam: Elsevier Science) chapter 163
[28] Talik E 1994 *Physica* B **193** 213
[29] Palewski T, Tristan N V, Nenkov K, Skokov K and Nikitin S A 2003 *J. Magn. Magn. Mater.* **258/259** 561
[30] Talik E, Mydlarz T, Kusz J and Böhm H 2002 *J. Alloys Compounds* **336** 29
[31] Saito A T, Tutai A, Sahashi M and Hashimoto T 1995 *Japan. J. Appl. Phys.* **34** L171
[32] Baranov N V, Markin P E, Mushnikov N V and Goto T 2001 *Mater. Sci. Forum* **373–376** 405
[33] Gignoux D and Lemaire R 1974 *Solid State Commun.* **14** 877
[34] Elliot R J and Wedgewood W A 1963 *Proc. Phys. Soc.* **81** 846
[35] Baranov N V 2004 *Phys. Met. Metallogr.* **98** (Suppl. 1) 10
[36] Gignoux D and Schmitt D 1991 *J. Magn. Magn. Mater.* **100** 199
[37] Gignoux D and Schmitt D 1993 *Phys. Rev.* B **48** 12682
[38] Ball A R, Gignoux D and Schmitt D 1993 *J. Magn. Magn. Mater.* **119** 96
[39] Irkhin Yu P, Rayevskaya L T and Abelskii Sh Sh 1977 *Fiz. Tverd. Tela* **19** 3363
Irkhin Yu P, Rayevskaya L T and Abelskii Sh Sh 1978 *Sov. Solid State. Phys.* **19** 1964 (Engl. Transl.)
[40] Lu Q F, Umehara I, Adachi Y and Sato K 1997 *Mater. Trans. (JIM)* **38** 1
[41] Fournier J M and Gratz E 1993 *Handbook on the Physics and Chemistry of Rare Earths* vol 17, ed K A Gschneidner Jr, L Eyring, G H Lander and G R Choppin (Amsterdam: Elsevier) chapter 115, p 409
[42] Sato N, Imamura K, Sakon T, Komatsubara T, Umehara I and Sato K 1994 *J. Phys. Soc. Japan* **63** 2061
[43] Stewart G R 1983 *Rev. Sci. Instrum.* **54** 1
[44] Taylor K N R and Darby M I 1972 *Physics of Rare Earth Solids* (London: Chapman and Hall)
[45] Cable J W and Nicklow R M 1989 *Phys. Rev.* B **39** 11732
[46] Nigh H E, Legvold S and Spedding S 1963 *Phys. Rev.* **132** 1092
[47] Fisher M E and Langer J S 1968 *Phys. Rev. Lett.* **20** 665
[48] Bouvier M, Lethuillier P and Schmitt D 1991 *Phys. Rev.* B **43** 13137
[49] Lounasmaa O V 1962 *Phys. Rev.* **128** 1136